

towards a sampling algorithm for Navier-Stokes, and potentially for the one dimensional heat equation: enforcing reliability of the sampling process with the numerical behaviors of example analytical solutions

Pete Rigas, pbr43

November 14, 2020

1 introduction

1.1 statement

at the initial point of time evolution fixed at one vertex of the box if one is to assume that there are **no** boundary conditions imposed, is a preliminary step towards introducing a finite differencing approach which can be used to solve several non linear problems of interest as discussed in **Lubasch et al.** In particular, couplings \mathcal{J}_{ij} in a Hamiltonian \mathcal{H} are constructed towards forming a probability measure so as to compare the likelihood of different configurations occurring within a sample space \mathcal{S} . From the discretization of the plane, the Brownian bridge sampling process is carried out at point depending on the variance δ , the number of steps \mathcal{N} of the bridge, and finally, the total time that the bridge spends within each box.

By contrasting the distribution of the random samples within a fixed box, and outside of a fixed box, we establish immediate connections between the short and long range interactions of the system. Through each \mathcal{J}_{ij} , the time evolution of turbulent flow is modeled under \mathcal{H} by:

- forming a sample array of the bridge values that are randomly assumed within a fixed $B_{x_i}^\epsilon$,
- determining the displacement of the bridge sampling at each neighboring point in the array by forming the pointwise difference between neighboring elements of the array,
- constructing the couplings within $B_{x_i}^\epsilon$, and outside of $B_{x_i}^\epsilon$, which are of the form $\mathcal{J}_{ij} = \frac{|t_i - t_j|}{\sum_{\text{Box}} t_k} \exp(-|x_i - x_j|)$, intentionally defined so that the turbulent flow between points that achieve a maximum distance away from each other in $B_{x_i}^\epsilon$ not only decays exponentially with respect to the Euclidean distance between the point, but also so that the long and short range couplings of \mathcal{H} can be formed by partitioning the sample array into the number of steps \mathcal{N} taken in each box of the discretization,
- computing \mathcal{H} , of the form $\mathcal{H} = \sum_{i \sim j: x_i, x_j \in B_{x_i}^\epsilon} \mathcal{J}_{ij} \cos(\theta_{\text{disc}}) + \sum_{i \not\sim j: x_i, x_j \notin B_{x_i}^\epsilon} \mathcal{J}_{ij} \cos(\theta_{\text{disc}})$, where the discrepancy angle is used to compute whether the Ricci curvature tensor $R(X, Y)Z$, for a well defined connection ∇ is satisfied,
- comparing the probability of different configurations occurring, dependent on the random samples of the bridge from a fixed frame of reference, with the law $\mathbf{P} = \frac{\exp(-\mathcal{H})}{\mathcal{Z}}$, where $\mathcal{Z} = \sum_{\text{Box}} W(t)$, where $W(t)$ is the continuous trajectory of the bridge

With the construct mentioned above and to be described in further detail below, it is possible to:

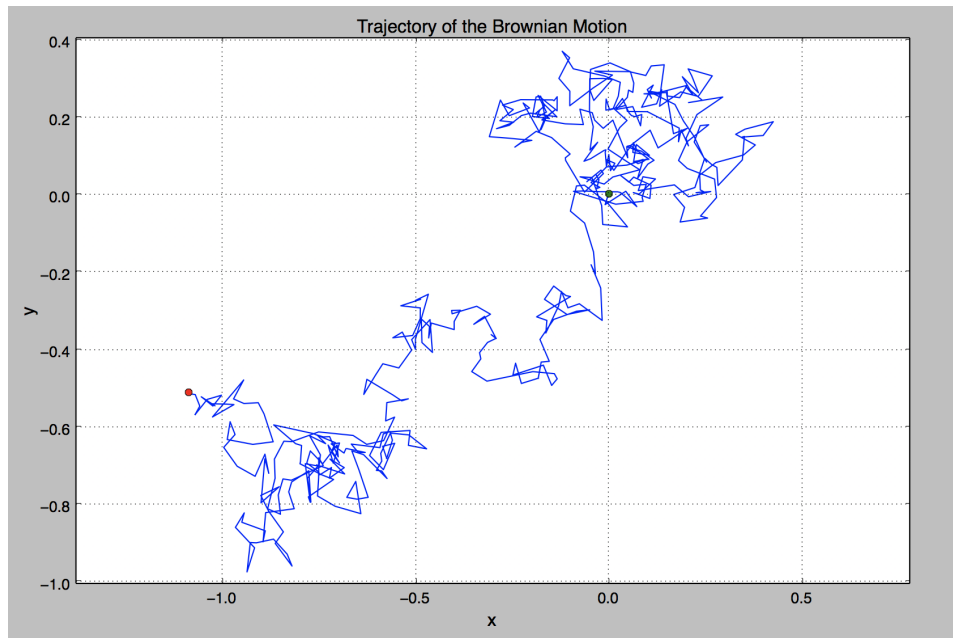
- Generate wider families of additive Gaussian noise whereby the evolution of the sample distribution can be continuously varied, so as to construct distinct measures $\mathbf{P}_{W(t)}^i$, where $W(t)$ is the bridge sampled at all admissible t , such that from each collection the samples can be used to predict the trajectory of solutions for Navier-Stokes in three dimensions for which closed formula of general analytical solutions are not known. The Brownian bridge in a 3 dimensional ambient space can be constructed by incorporating an additional degree of freedom for the random motion, corresponding to another spatial variable.

- From Otarod & Otarod, 2011, solutions are obtained for constant pressure, or also for spatially varying pressure of the form $p = \beta x - \alpha y$, with the analytical form of such solutions can be constrained either geometrically through cells of a discretization that are physically occupied by an object around which the pressure distribution is to be computed, or by analytic criteria on the particular subset of the plane over which the equation is to be solved.
- More generally, the bridge process will also elucidate how to obtain cost functions for other equations that share in properties of diffusion that the Navier-Stokes equations exhibit for incompressible fluid flow. With solutions to the one dimensional heat equation, an adaptation to the steps given below will be carried out so as to modify collections of the bridge samples at only a countable number of points in the random collection, from which cost functions for each equation will be obtained, dependent on the mean and variance needed to specify sampling distributions, or subdistributions.

2 background

3 implementation

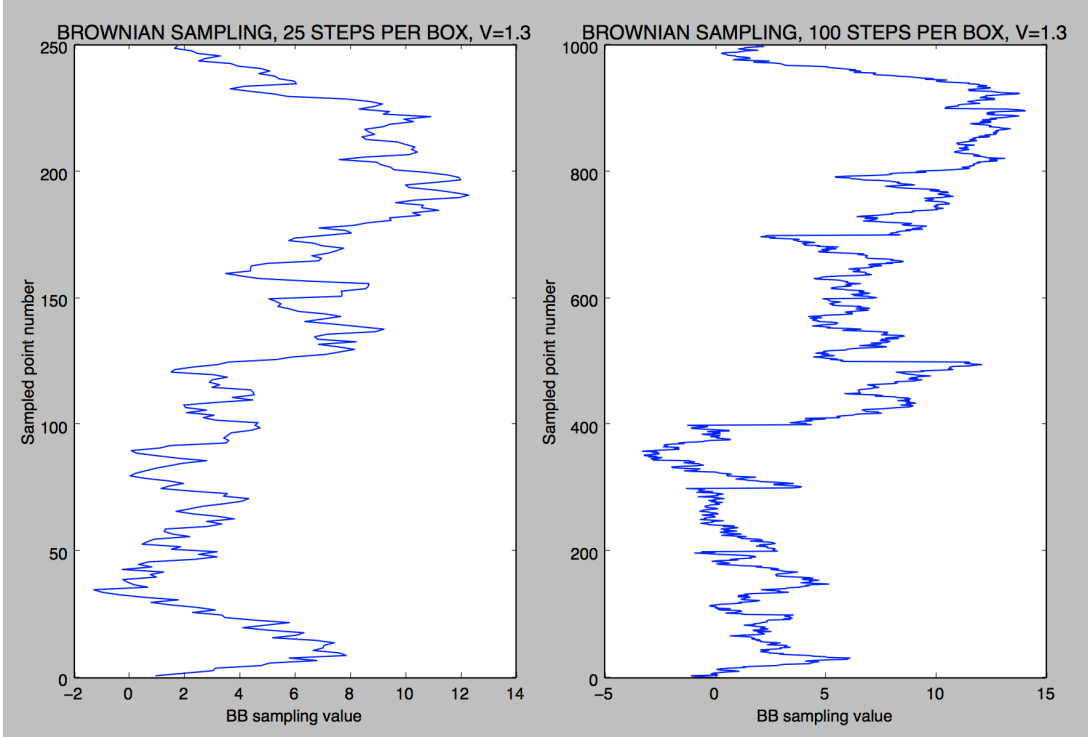
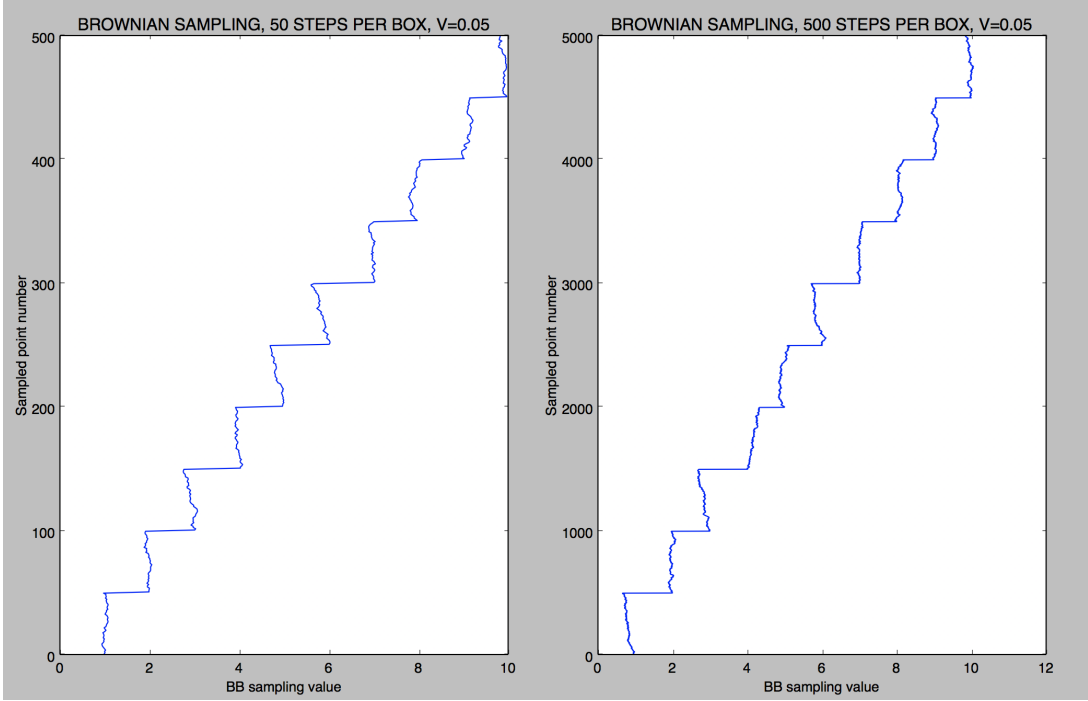
Bridge sampling takes place in the plane without enforcing any discretization. In this most simple case, the sampling would take place at one fixed initial point, and would end at another fixed final point, with a determinable number of steps of the sampling process, in addition to the total time during which the sampling process would occur.



(ABOVE) The sampling process with the beginning and ending points demarcated in blue, and green, respectively.

Besides the most simple case shown above, it is also natural to ask how the bridge sampling would behave with respect to the discretization of the grid. Namely, if we were to enforce a grid discretization over which grid points are used to sample the bridge, would the bridge reflect the irrotational symmetry of a random walk that would have a very high probability of visiting multiple points of the grid on **several** occasions?

To demonstrate more recent progress in the past few weeks to address the parameter regime under which the bridge sampling would visit each point of the discretization nearly once, so as to prevent having multiple values in the sample collections with the same coordinate values, the plots below demonstrate comparisons between more, and less, optimal choices under which the variance δ can be numerically adjusted.



(ABOVE) Plots of the bridge values achieved from the sampling process for a fixed number of steps and variance. In the first plot, the sampling process has 50, and 500 steps per box over the interval $[1, 10]$, which itself is partitioned into 10 equidistant segments, each with a variance of 0.05. In the second plot, the sampling process enacted with 25, and 100, steps per box, with a fixed variance of 1.3, which significantly, is greater than the side length $\epsilon \equiv 1$ of the boxes in the grid discretization.

overview of the strategy

We will break up applications of the strategy by looking at the behaviors of the analytical solution to Navier-Stokes, in correspondence to the behavior of the sampling, particularly to determine whether the

sample distribution noticeably varies through continuous adjustment of the mean, variance and number of steps of the motion.

Before giving a broader discussion, the simulations below examine different choices of the real parameters in the solution

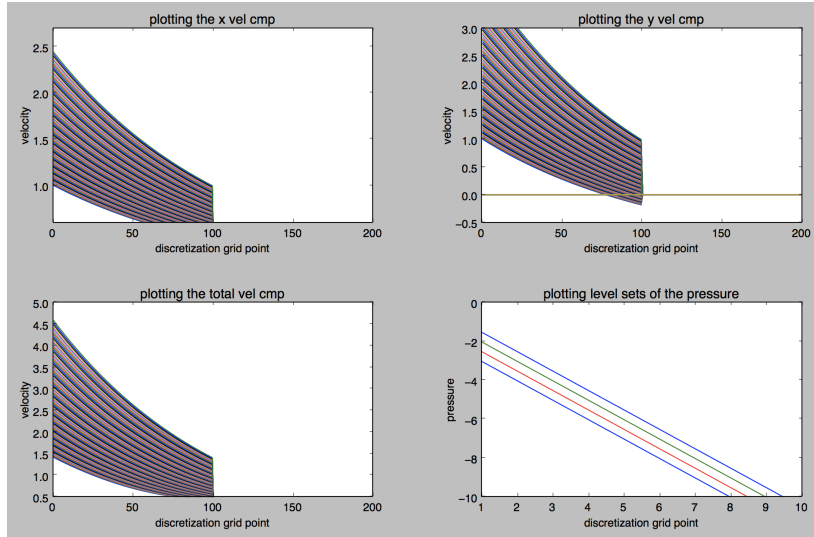
$$u = A \exp\left(\frac{c}{\nu(\alpha^2 + \beta^2)}(\alpha x + \beta y)\right) + B ,$$

for the x component of the velocity, and

$$v = \frac{1}{\beta} \left(c - \alpha B - \alpha A \exp\left(\frac{c}{\nu(\alpha^2 + \beta^2)}(\alpha x + \beta y)\right) \right) ,$$

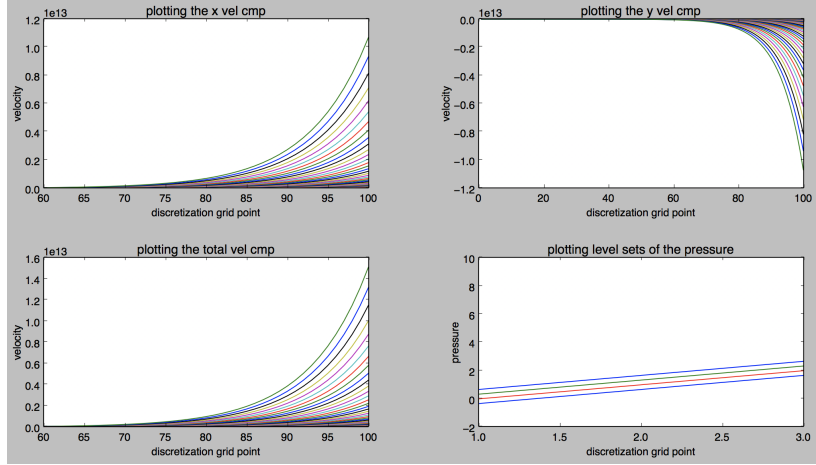
for the y component of the velocity.

3.1 Case 1: comparison of the behavior of the bridge sampling to the behavior of the analytical solution for disagreeing sign choices of α and β



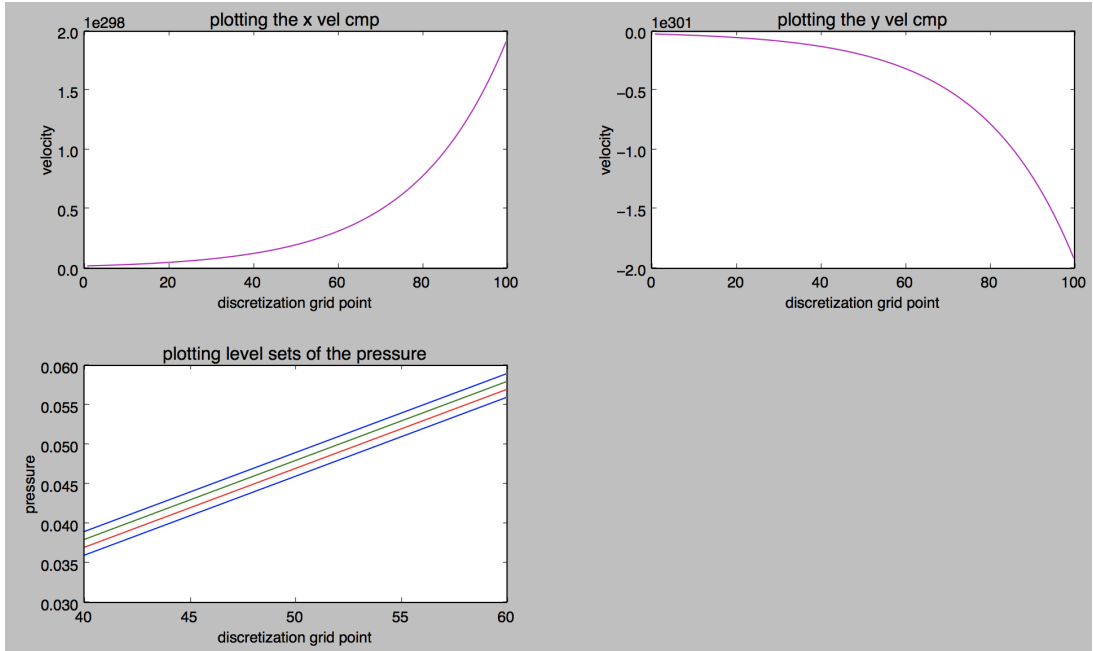
(ABOVE) The first three plots above exhibit the spatial dependence on the x and y components of the solution. As expected, given function evaluations across varying x for fixed y corresponds to level sets of the multivariable function shown in the fourth plot, a hyperplane. In all of the plots above, the colors of each different ray that are plotted demonstrate how the x component of the velocity in the first case of the analytical solution given capture the behavior of the pressure distribution which influences the incompressible fluid flow at every spatial point. Instead of having to sample the analytical solution at each and every point of the discretization, we will instead allow the sampling process to run for the complete number of steps which I have taken in my code to be 50. With any arbitrary number of steps within each box, the probability of the bridge to transition to this point, if the pressure distribution in this subset of the plane is disproportionately higher than in other subsets over which a solution is determined, will be distributionally penalized.

3.2 Case 2: comparison of the behaviors for agreeing sign choice of α and β



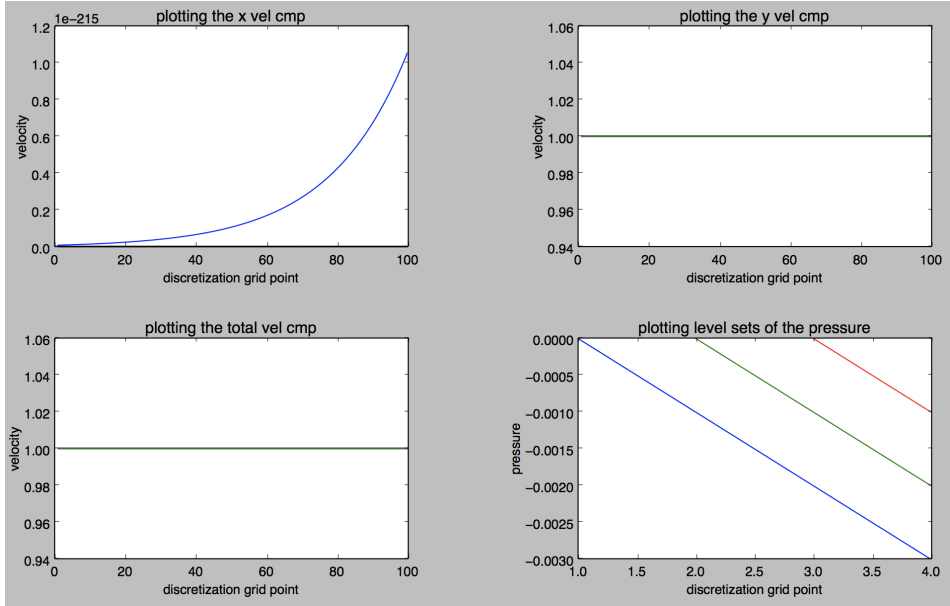
(ABOVE) As a simpler case, the signs of agreeing α and β together impact the behavior of the velocity spatially, almost equally. As in the previous plot, a few neighboring level sets of the hyperplane projected down to a line in the plane are shown.

3.3 Case 3: comparison of the behaviors for agreeing sign choice of α and β , disproportionate in magnitude



(ABOVE) In this case, we have disproportionately favored β in our choice of a free parameter for the given analytical solution for the u and v components of the velocity. As expected, we encounter that both terms contribute strongly towards the total velocity that we observe in each degree of freedom. Furthermore, we observe that the x velocity and y velocity each start at 0 at the first spatial pair and monotonically increase, and decrease, respectively.

3.4 Case 4: comparison of the behaviors for equal in magnitude, disagreeing sign choice of α and β , largely disproportionate in opposing α



(ABOVE) If we strongly bias one of the coefficients from which we study the pressure distribution with respect to movement amongst variables in the ambient space, that component of the velocity is more dominant than over the remaining component. Hence the dot product of the position vector and the vector field for the pressure is largely resemblant of the orientation of the pressure gradient.

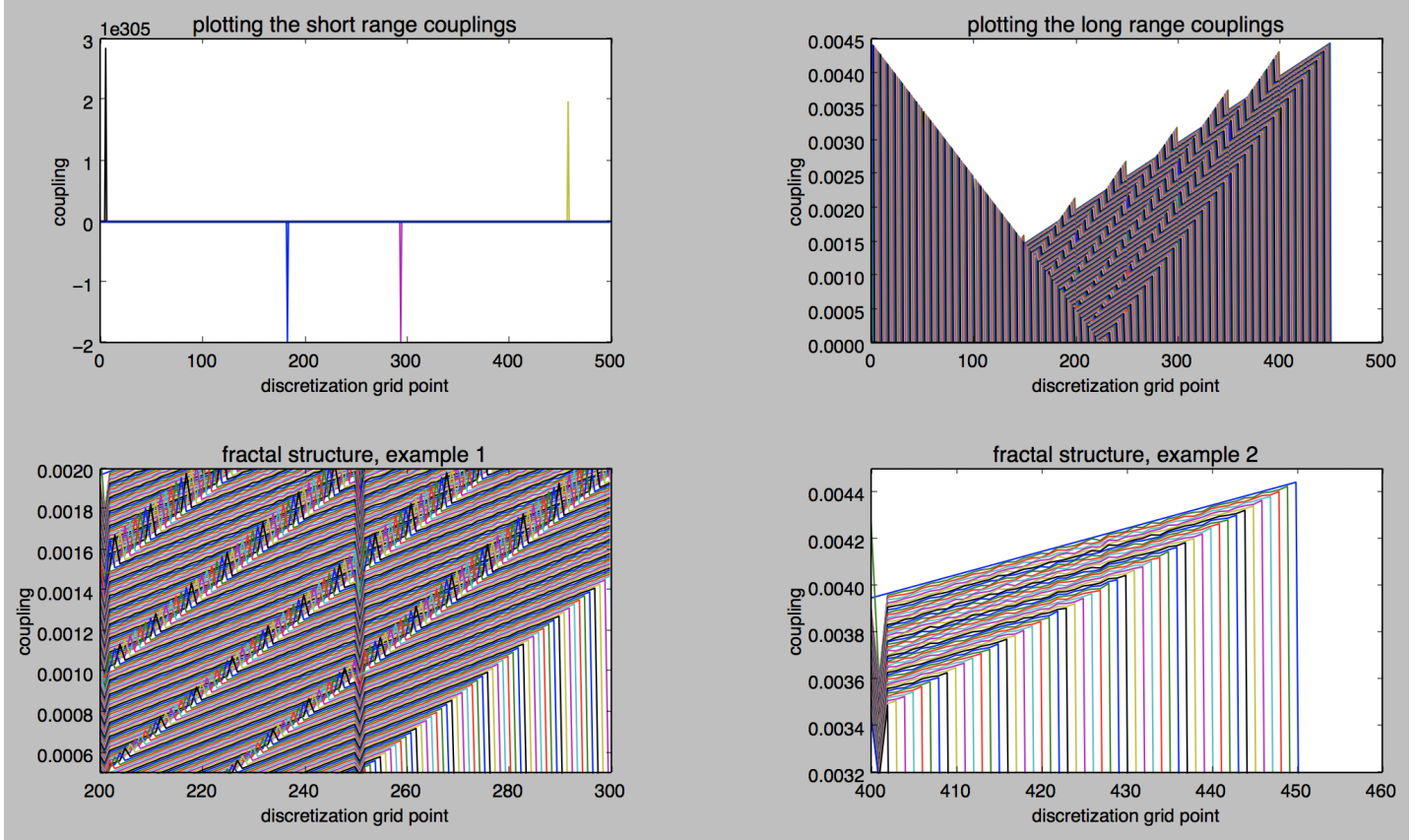
3.5 upshots of the numerics

but also so that more complicated distributional patterns within each collection of samples can be accounted for to reflect the rough numerical behavior of *each* pressure distribution.

To further elucidate that the variance of the sampling process detrimentally impacts the values assumed by the sampling process, moreover, that the variance should be chosen to be strictly less than the unit length of each box in the discretization, the second plot in the series above demonstrates that the bridge retraces values that it already assumed with high probability as the variance of the sampling process increases past the unit length of the discretization.

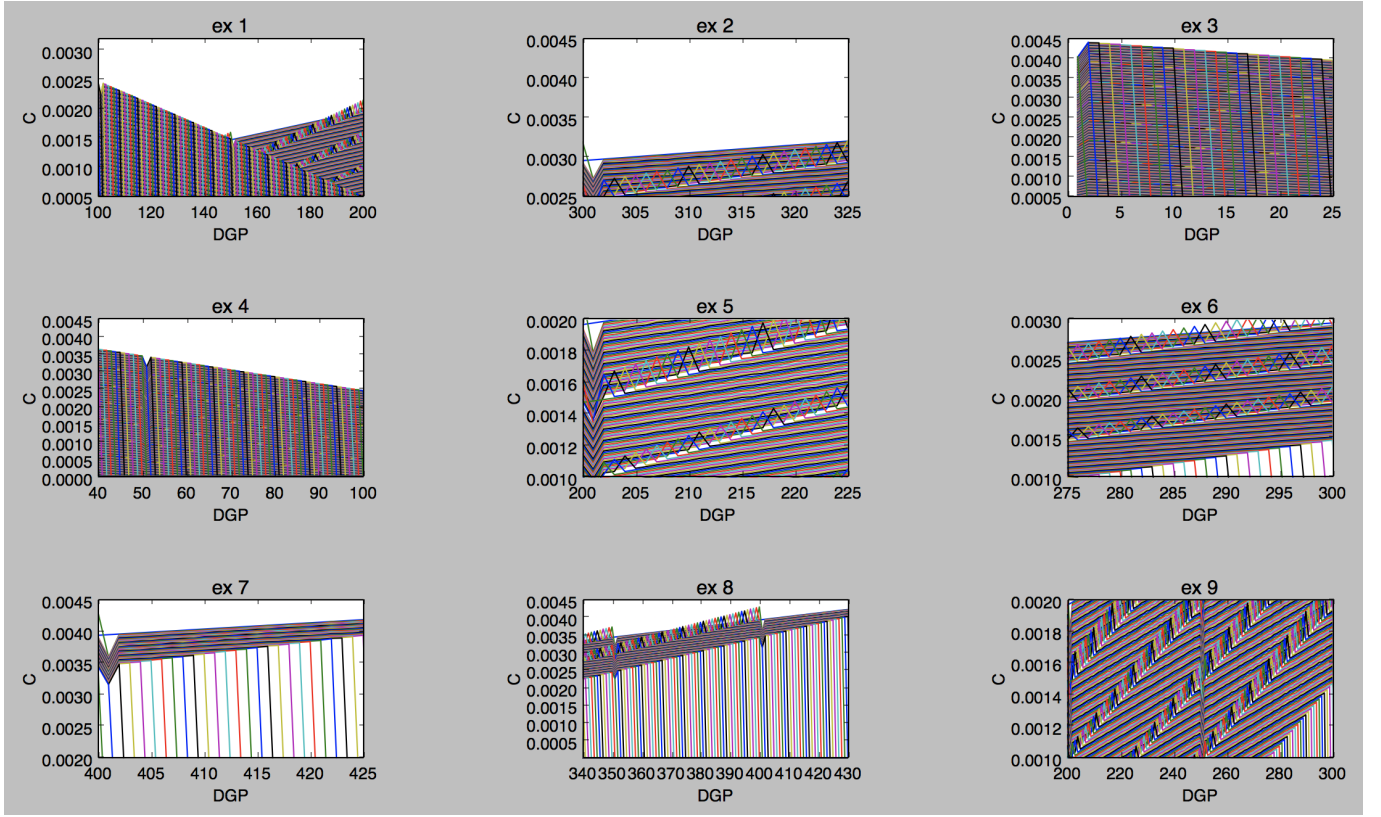
Besides collecting the values of the bridge sampling, it is also useful to visualize the average displacement of the sampling process at each point during which a sample is collected. Through a specific initialization scheme of each collection of 50 samples from the mean, variance and number of steps that are initially passed onto the Brownian bridge which is described below for the long and short range coupling plots within and outside of some fixed box of the discretization, long and short range couplings are related to the free energy of the system, which is directly proportionate to the summation of all bridge samples, and can be easily represented by plotting the summation of all bridge samples after a given time step on the log scale. By making use of the long and short range couplings in a Hamiltonian whose form is deliberately composed not only of exponentials to penalize the probability of having long range interactions within the system, but also of the displacement between angles at which the random edges are oriented, relative to the time axis or any fixed ray from the origin, from which we may calculate the difference between covariant derivatives. Algorithmically, this can be achieved by following the steps given in **Section 3** for the graph algorithm, in which distance between identical vector fields that only differ at the point of unacceptable disagreement between the bridge sample and the analytical solution evaluated at the same spatial position have its *displacement angle* computed. Between subsequent bridge samples, if there is a large jump, θ_{disc} is conditioned so that one can numerically determine the extent Ricci curvature symmetry is broken or preserved, which given our previous plots of the pressure distribution for 4 cases of α and β , can be achieved by calculating the weight of different paths as they are undergone by the bridge, where the contours γ_1 and γ_2 consist of a random permutation of the bridge samples before the final time stamp at which the sample

is collected. With further developments towards a discussion of how to parameterize θ of the rotation gate. Geometrically, being able to visualize and construct the curvature of a manifold whose open covers are level sets of the bridge sampling in the plane can readily lead up to a scaling of the sampling processes in three dimensions, from which approaches to obtaining good readouts can be implemented, which is one of the main motivations for the approach in which there are no analytical solutions to Navier-Stokes for a specified pressure distribution, or in higher dimensions.



(ABOVE) The plots exhibit behavior of the short and long range couplings for the Hamiltonian. In the first plot, the short range couplings, of the form given in the first page of the report, are plotted. As a future direction, the author would like to continue devoting attention towards an expression for the couplings that are more numerically stable, as the long range couplings are. In the second plot, the behavior for the long range couplings is plotted with its accompanying grid point number. To briefly reiterate portions of the code, we are solving for the Naiver-Stokes equations over $[0, 10]$, and with the bridge sampling process we construct long range couplings for all of the samples that are outside of the fixed box of reference from which we are running a disjoint process. With 50 steps per box and 10 boxes in the discretization each with unit length, the remaining 450 samples out of the 500 total have a normalizing time, which I have denoted the long time sum, of the form $\mathcal{J}_{ij} = \frac{|t_i - t_j|}{\sum_{\text{outsideBox}} t_k} \exp(-|x_i - x_j|)$. The third plot above demonstrates a zoom in of the regions of the long range coupling environment produced above, in which the long range coupling sequences are individually plotted in distinct colors. From each color, we observe that the long range couplings behave in quite a peculiar way, and were initially constructed so as to reflect the underlying distribution of the sampling process itself. That is, if we examine the yellow line throughout the entirety of the third plot, we observe that that from any one of the rays, beginning at $x \approx 200$ and ending at $y \approx 0.0020$, there are a determinable number of maxima of the yellow curves that peak at higher amplitudes as points are taken further down the sampling process. In the fourth plot, another zoom in is shown of the self similar structure of the surface plotted from the long coupling constants, in the sense that along the diagonal line beginning from $x \approx 400$ and monotonically increasing until $x \approx 450$, different rays of the long coupling constants increase to a saturation value determined by the height of the diagonal, and them sharply decrease. For construction of the Hamiltonian, plots of behavior of the long range couplings demonstrate that the long range couplings for discretization points that have successively higher x , or y , values captures a

similar spatial dependence that earlier plots of the pressure distribution reveal for exponentially increasing, or decreasing, solutions to Navier-Stokes.



(ABOVE) Each entry in the plot above demonstrates more of the self similar, fine grained behavior in the long range couplings plot. In the **first** subplot, a portion of the long range couplings surface exhibits a collection of couplings for which the bridge samples are inversely proportional to the grid point that is sampled, as the number of points increases. In the **second** plot, another portion of the surface exhibits the couplings at which different curves, whether colored **yellow** or **blue**, reach a fixed maximum coupling constant which is dependent on the nature of the underlying sampling distribution. In the **third** plot, another perspective of the decay of the long range couplings is shown, in the **yellow** line which intersects the axis around the 5th discretization point sharply decays in the magnitude of its coupling as the same process proceeds to draw the 5th random variable. In the **fourth** plot, a similar pattern at the number of discretization point at which the **yellow**, and any other colored lines approach 0 is observed. In the **fifth** and **sixth** plots, zoom ins of the peaks of each long range coupling constant sequence from the **second** plot is given. In the **seventh** plot, the long range couplings numerically decrease in a similar manner as given in the **fourth** plot, but experience a sharp decay after the 400th discretization point. In the **eighth** plot, the maximum of the triangular interfaces increase monotonically with the discretization point, and approach 0 at a later time. In the **ninth** plot, the portion of the long range couplings surface in **between** the maxima of every color line is achieved. In fact, after achieving the maxima, upon close examination one can see that the **yellow** lines continue to increase as the grid discretization point number increases, and then approach to 0 after a sufficient number of samples has been drawn. As previously mentioned, for the initialization step of the algorithm,

From numerical simulations of the bridge across the interiors of distinct boxes in our running example of the uniform discretization of $[1, 10]$ with $\epsilon \equiv 1$, the methodology is capable of producing a random environment by incorporating the behavior of bridge sampling to the diffusion process of air spreading throughout a subset of the plane under a known pressure distribution. However, for one point of future work, the methodology is also capable of linearly modifying a collection of bridge samples as follows. First, we construct the initial sampling sequence from the bridge without enforcing conditioning that the sampling process remain within a specified error bound of the value of the analytical solution that were introduced earlier, which are precisely Cases 2.1 and 2.2 from the 2011 paper. Then, from such example analytical solutions to the equation, once the first sampling distribution has been substantiated, to construct the next

distribution in the sampling collection if additional refinements in the behavior of the sampling are necessary, find the earliest time t_j at which the bridge differs by more than arbitrary $\epsilon > 0$ from the accompanying value of the analytical solution. At this time, all members of the sampling distribution before t_j are populated in the same positions that they occupied in the succeeding sampling collection, but the sampling process is undergone repeatedly from this point forwards, with knowledge of the value of the analytical solution at the position of mismatch. With at most $|t_j - t_N|$ executions for N steps of the bridge, construct each remaining sampling collection within the family by determining the next largest time past t_j at which the bridge sample differs from the analytical solution by more than the same prescribed difference. Repeat the procedure for each instance of this type.

Through admissible refinements of the sample collections, the arguments that follow will demonstrate how to extend the sampling process to 3 dimensions for Navier-Stokes,

To improve upon ...

In a similar way that many current efforts for the one dimensional heat equation are towards constructing an ansatz that spans a considerable region of the Hilbert space

can identify a random Fourier series representation of the bridge that not only most accurately adheres to the behavior of the solution, but is also able to achieve a suitable basis from

towards analyzing a wider class of pressure distributions and velocities along each basis element

region of the Hilbert space that the random Fourier series is spanning, which can be generated from the bridge samples that I have used to construct plots previously given in the report.

3.6 warming up the algorithm: inspecting vertices within $B_{x_i}^\epsilon$

First, we begin our implementation from some fixed $v_i \in B_{x_i}^\epsilon$. From this fixed initial point and accompanying collection of times t_i on which the Brownian sampling is begun, define an arbitrary threshold parameter ϵ . After searching through nearest neighbor samples of the Brownian sampling distribution, collect all pairs of samples $W(t_i)$ and $W(t_j)$ for which $|W(t_i) - W(t_j)| < \epsilon$, satisfying $|t_i - t_j| = 1$.

Second, edges of the lattice graph will be completed as follows. For each instance in which we encounter a pair of nearest neighbor samples (see the conditions above) for which $|W(t_i) - W(t_j)| < \epsilon$, fill in an edge between x_{t_i} and x_{t_j} , with length $|W(t_i) - W(t_j)|$.

After repeating the previous 2 steps above indefinitely depending on the distribution of samples, and cardinality of total times t during which samples are drawn, one can identify the subregions of the plane for which the highest density of edges will occur, which is determined not only on the total number of instances for which the algorithm finds that the nearest neighbor sample difference is less than ϵ , but also on the length between the nearest neighbor samples, both of which are dependent on the variance δ of the Wiener process.